*Pooja Singh[a,b], Avshish Kumar[a], V. K. Jain[a]

[a]Amity Institute for Advanced Research and Studies (Materials & Devices), Amity University Uttar Pradesh, Noida, India.
[b]Maharaja Surajmal Institute of Technology, New Delhi, India.

Scientific paper
ISSN 0351-9465, E-ISSN 2466-2585
https://doi.org/10.62638/ZasMat1263

Zastita Materijala 65 ( )
(2025)

Development of UV Photodetector using SnO_2/AuNPs@SiNWs heterojunction on Si chip

ABSTRACT

In this study, we present the development of a hybrid nanostructure based on silicon nanowires (SiNWs) and tin oxide (SnO_2) and Au nanoparticles, which was utilized to develop a UV photodetector. Metal assisted chemical etching (MACE) was used to create SiNWs on p-Si (1 1 1) substrate, while reduction synthesis and co-precipitation techniques were used to create AuNPs and SnO_2 nanoparticles, respectively. These AuNPs and SnO_2 nanoparticles were then deposited on top of SiNWs. Using an X-ray diffractometer (XRD), UV-Visible spectrophotometer, and scanning electron microscopy (SEM), the synthesized SnO_2/AuNPs@SiNWs hybrid nanostructure was examined. The synthesized SnO_2 nanoparticles were subjected to TEM examination as well. At room temperature, the UV photocurrent response of SnO_2/AuNPs@SiNWs was studied at varying UV light intensities as 1, 1.5, and 2 mW/cm^2. The hybrid nanostructure of SnO_2/AuNPs@SiNWs was found to have a photocurrent response time to be very fast (1.32 s). As we turned off the UV source, the sensor reached to its initial state in ~0.77 s. The sample was checked continually for three on/off sets of illumination at a regular interval of 60 s. Therefore, the work disclosed here has great promise for the advancement of highly effective miniature UV photodetectors with unique features.

***Keywords**: Photodetector, Ultra-violet, Gold Nanoparticles, Silicon Nanowires, Tin oxide.*

1. INTRODUCTION

A device that transforms light energy into a measured electrical reaction is called a photodetector (PD). All solid state photodetectors operate on the same fundamental concept. When a photon with enough energy interacts with a semiconductor material, the distribution of electron energies within the material is momentarily altered[1,2]. An electron can become energetically conducting when it has enough energy to do so, allowing it to freely move within the crystal. A vacancy, or hole, is left behind by the migrating electron and is free to move within the crystal. They are together known as electron hole pair and in photodetector, one such pair is created for every absorbed photon. If the electron hole pair left in material long enough, they will recombine and give up extra energy in the form of heat. The time scale during which it happens is called recombination lifetime, τ_r. While excited, the electron and hole will drift in the presence of an electric field, creating electric current. This current can be detected by connecting the active area of the semiconductor into an electric circuit. Here, however we are specifically interested in PDs for the detection of UV wavelength [3, 4].

UV PDs find wide applications in various fields like industrial, environmental, military and commercial fields[5]. In the domains of solar astronomy, water sterilization, flame detection, and safe space communication, they are frequently employed to detect UV light [6, 7]. Particularly, UV PDs have garnered a lot of attention lately because of the growing demands from the military and civic sectors to develop UV equipment that can function in high temperatures [8]. Commercially available PDs are utilized in various applications such as atmospheric clock transfer using femtosecond frequency combs, measuring speckle motion to monitor ultrasonic vibrations, measuring the polarization state of a weak signal field by homodyne detection, and remote optical diagnostics of non-stationary aerosol media in a wide range of particle sizes [9].

*Corresponding author: Pooja Singh
E-mail: *psingh126@gmail.com*
Paper received: 16. 09. 2024.
Paper accepted: 02. 12. 2024.
the website: https://www.zastita-materijala.org/

There are three bands in the UV spectrum. Three wavelength ranges are identified: UVA, UVB, and UVC. The wavelength range from ~ 320 nm to 400 nm is assigned to the band UVA, while the wavelength range from 280 nm to ~ 320 nm is assigned to the band UVB and the wavelength range from 100 nm to 280 nm is assigned to the band UVC[10]. UVA makes up 95% of the UV light that reaches the earth and is located in the visible region among these bands.

In this investigation, we developed a silicon nanowire-based heterojunction p-n device. The devices obtained as a p-n heterojunction may give photodetectors functioning in a larger wavelength range due to the wavelength constraint of silicon homojunction in terms of photodetector performances. Moreover, heterojunction photodetectors are created by combining several materials with nearly matched lattice characteristics but distinct band gaps [11]. This absorbs various wavelengths, enabling the photodetector to be employed in a broad spectral range. There are opportunities for high-performance photodetectors using lattice-matched heterojunctions. As a result, creating p-n heterojunctions is frequently more advantageous than creating homojunctions since they are cheap, simple to fabricate, and have good performance. In optical devices, metal oxide semiconductors play a crucial role because of their intriguing optoelectronic features.

The wide gap semiconductors for example, *SnO_2* [12]*, GaN* [13]*, Ga_2O_3* [14]*, TiO_2* [15]*, ZnMgO* [16] and *ZnO* [17], are attracting significant research and commercial owing to their improves thermal stability, high breakdown voltage, low cost and favourable sensitivity to UV radiation. Here, in this work we choose SnO_2 nanoparticles which is a wide band gap semiconducting material. SnO_2 found interesting electrical and optical application. MSM UV photodetectors based on SnO_2 have been demonstrated recently, but they have a lot of issues. Interstitial Sn atoms, numerous oxygen vacancies, and other defects are common in SnO_2 material. These flaws provide a huge amount of background carriers, which in turn cause a high dark current. Another reason is that some of these defects function as trap centers, which prevent photogenerated electrons and holes from recombining, slowing down the response time[12]. But the forbidden dipole transition among its valence band and conduction band limits its applicability in photodetectors. The performance of UV PDs enhances with incorporation of nobel metal nanoparticles due to the generation of Localized Surface Plasmon Resonance (LSP). LSP encourages the confinement of optical fields directly affecting the increase in the intensity of the optical energy inside the SnO_2[18]. This lead to better optical and electrical performances of the photodetector. Keeping in view above considerations, for the first time, we have used AuNPs/SnO_2 heterojunction for UV detection and experimental data depicts good results that to the best of our knowledge has not been reported so far by this nanostructure.

2. EXPERIMENTAL WORK

2.1 Materials Procurement

For the synthesis of SiNWs, hydrogen peroxide (30%), hydrogen flouride(40%), IPA(99%) were purchased from Rankem, Fisher Scientific SRL respectively. Sulphuric acid (99%) and nitric acid procured from Merck. Silver nitrate (99.9%) was procured from Qualikems. For the synthesis of Gold nanoparticles, gold hydrogen chloride acquired from Sisco Research Laboratories pvt. Ltd. and trisodium citrate dehydrate (98%) from Loba Chemie Pvt. Ltd and for the synthesis of SnO_2 NPs, Tin chloride dihydrate $SnCl_2.2H_2O$ (98%, Sigma Aldrich), ammonia hydroxide (NH_4OH), Hydrochloric acid (HCl) and distilled water. The chemicals were used without any further purification.

2.2 Synthesis of SiNWs on Si chip

We choose n-type Si substrate and ultrasonicated it 10 mins with DI water, 10 mins with acetone and 10 mins with isopropyl alcohol to remove dust and oxides layer deposited over substrate. The substrate was then dipped in piranha solution (H_2SO_4:H_2O_2) taken in the ratio of 3:1 for 30 mins to remove organic and inorganic contaminations. Further cleaning the substrate by dipping in HF solution (1ml HF+9ml DI) for 2 mins, after HF dip the substrate was dipped in etching solution. Etching solution was prepared by ultrasonicated $AgNO_3$ solution (0.068g $AgNO_3$ + 20 ml DI) with HF solution (4ml HF + 16 ml DI). We kept the substrate in etching solution for 1 hour at 60°C [19, 20]. The length of SiNWs can be adjusted by changing the time for which we kept in etching solution. After that it is cleaned with HNO_3 solution for 5 mins to remove the Ag from the Si wafer. The oxidation-reduction takes place which is explained below.

$$Si(s) + 4Ag^+ + 6HF \rightarrow 4Ag(s) + 4H^+ + H_2SiF_6$$

2.3 Synthesis of AuNPs

In a typical AuNP synthesis [21], 20 ml of 1.0 mM gold hydrogen tetrachloride solution was prepared in a flask. Independently, 2mL of (1.0 wt %) trisodium citrate dihydrate solution was prepared. Using a hotplate, the flask holding the $HAuCl_4$ solution was heated while being vigorously

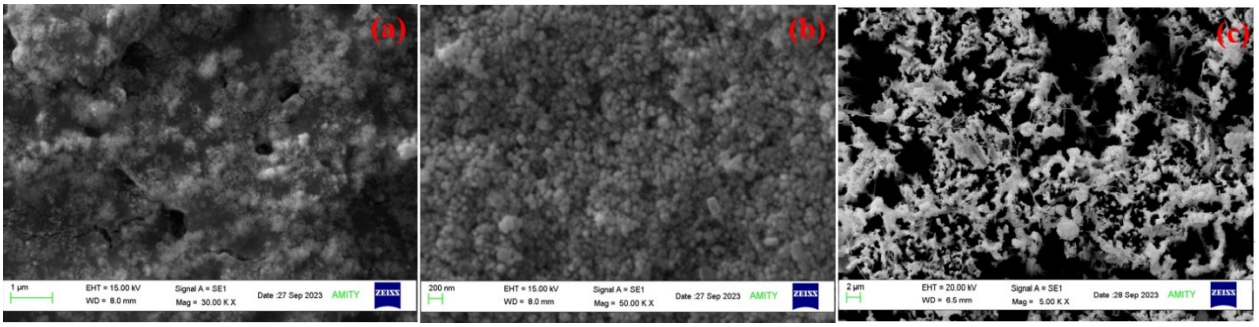

***Figure 1**. (a) Top view of SnO_2 deposited over Si substrate, (b) Top view of AuNPs deposited over Si Substrate, (c) Top view of SnO_2/AuNPs deposited over SiNWs.*

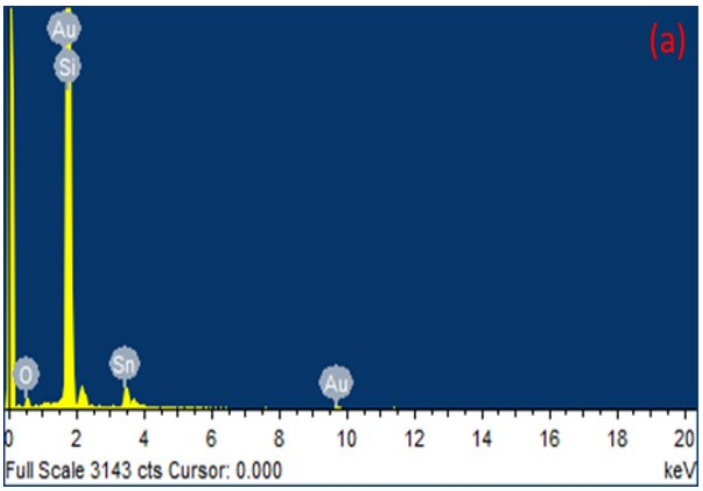

(b)

Element	Weight%	Atomic%
O K	9.08	17.91
Si K	68.90	77.47
Sn L	10.32	2.75
Au M	11.71	1.88
Totals	100.00	

***Figure 2**. (a) EDX spectrum of SnO_2/AuNPs@ SiNWs, (b) Atomic percentage*

and continuously stirred. A disposable Petri dish was utilized to cover the flask during the synthesis to prevent contamination and solvent evaporation. A 2 mL solution of citrate was quickly injected into the $HAuCl_4$ solution after it had reached the boiling point at room pressure. The main variable that was regulated to produce the appropriate particle size was the molar ratio of citrate to gold chloride. When the suspension turned wine red, the synthesis was finished. Depending on the molar ratio, the reaction typically took two to five minutes. The sample reached room temperature by natural cooling.

Here, gold ions react with citrate ions to form gold atoms as well as citrate acting as a reducing agent in producing the gold atoms. Citrate ions acts as shielding agent, wrapping around the cluster of atoms which constitute the nanoparticles[22]. This electrostatic sheath prevent agglomeration and stabilizes the particles.

2.4 Synthesis of SnO_2

The SnO_2 NPs were prepared by co-precipitation [23] technique where 0.85 g of $SnCl_2.2H_2O$ was added into 100 mL of ethanol in a 500 mL beaker with continuous magnetic stirring for 1 hr to obtain a homogeneous solution. 100 mL of hydrochloric acid was then added drop wise with further stirring the solution for another 30 min to get proper mixing the solution in a clear transparent form. Further, NH_4OH was added drop by drop till the pH of the solution became 8.5 where a milky white solution was obtained. This solution was kept on continuous stirring for 3 hrs. Thereafter the stirring was stopped and the solution was then washed with DI water as well as ethanol multiple times so that the residual chlorine content can be removed. The resulting solution was filtered, covered and left overnight for drying. The dried powder was then calcinated at 650^{o}C.

Then we ultrasonicate the solution of AuNPs and SnO_2 and then we drop casted the solution over SiNWs on Si chip and placed on PCB for making electrodes respectively.

3. CHARACTERIZATION TECHNIQUE USED

To study the stoichiometry, morphology, and structural analysis of the developed materials (SnO_2, AuNPs and its heterojunction nanostructure over SiNWs) various characterization techniques were used. Scanning electron microscope (SEM) of Zeiss (model: EVO-18) equipped with energy

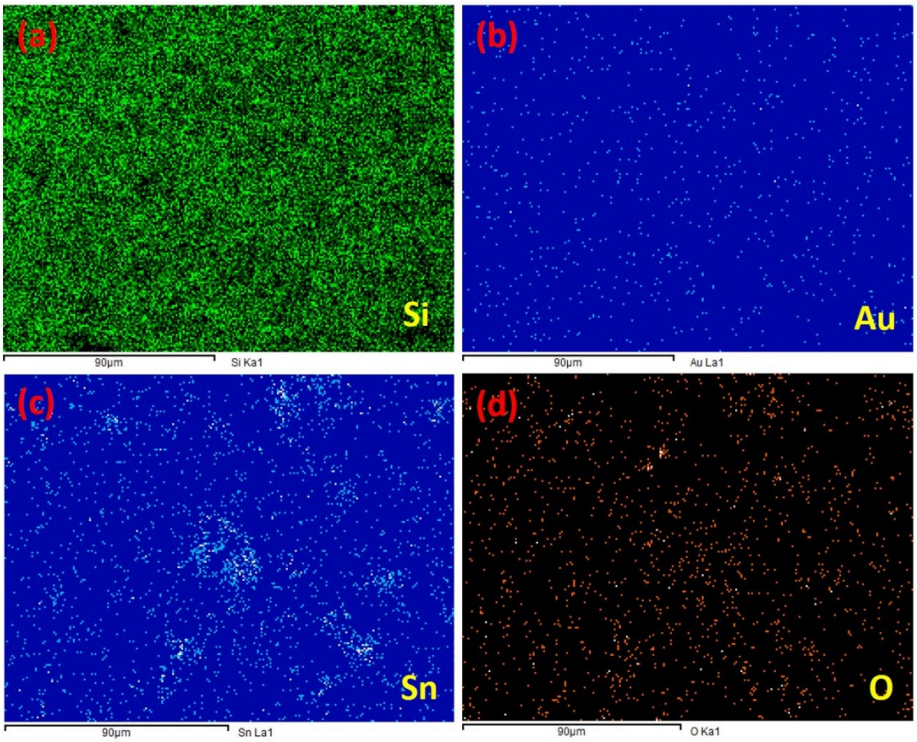

Figure 3. *EDX colour mapping of (a) Silicon (b) Gold (c) Tin (d) Oxygen*

dispersive X-ray spectrometer (EDS) was used to analyse the shape and size of the prepared nanostructures. Transmission electron microscope (TEM) of (JEOL, model no. JEM-2100G) was used to get the structural analysis. For the crystallographic analysis of the heterojunction nanostructure, Ultima IV PXRD (source Cu, K = 1.54Å) X-ray diffractometer was performed. UV–Vis spectrophotometer was also used to get the absorption spectra of the SnO_2, AuNPs and SnO_2/AuNPs. For UV sensing analysis, Keithley electrometer was used to record the data.

4. RESULTS AND DISCUSSIONS

4.1 SEM Analysis

The surface morphology of the developed materials was recorded using SEM and results were analysed. The top view micrograph of SnO_2 deposited over Si substrate has been depicted in Fig. 1(a) which clearly indicates uniform coverage of the substrate. Fig. 1(b) reveals the synthesis of Au nanoparticles whose particle size is in the range of 30-50 nm. Fig. 1(c) show the AuNPs and SnO_2 deposited over SiNWs. The micrographs showed the good coverage and a heterojunction between SnO_2/AuNPs and SiNWs.

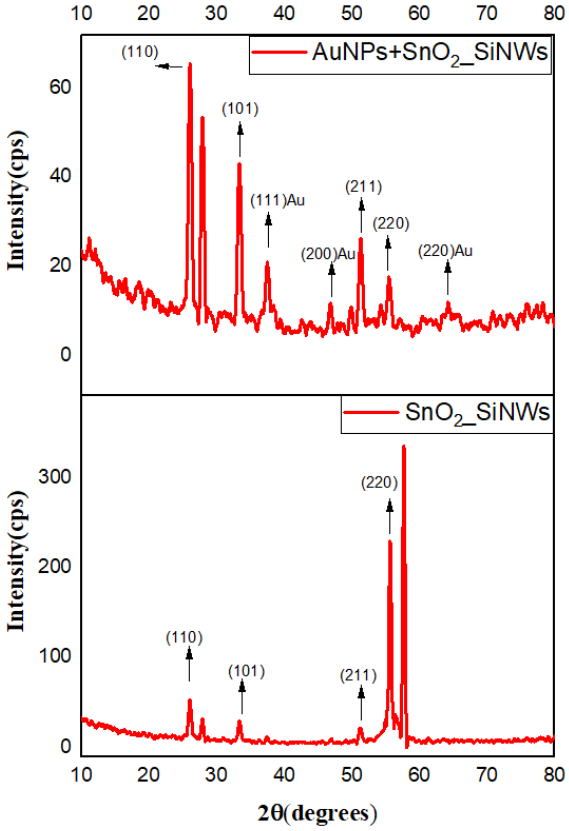

Figure 4. *XRD of SnO_2 and SnO_2/AuNPs deposited over SiNWs on Si chip is shown in (a) and (b) respectively.*

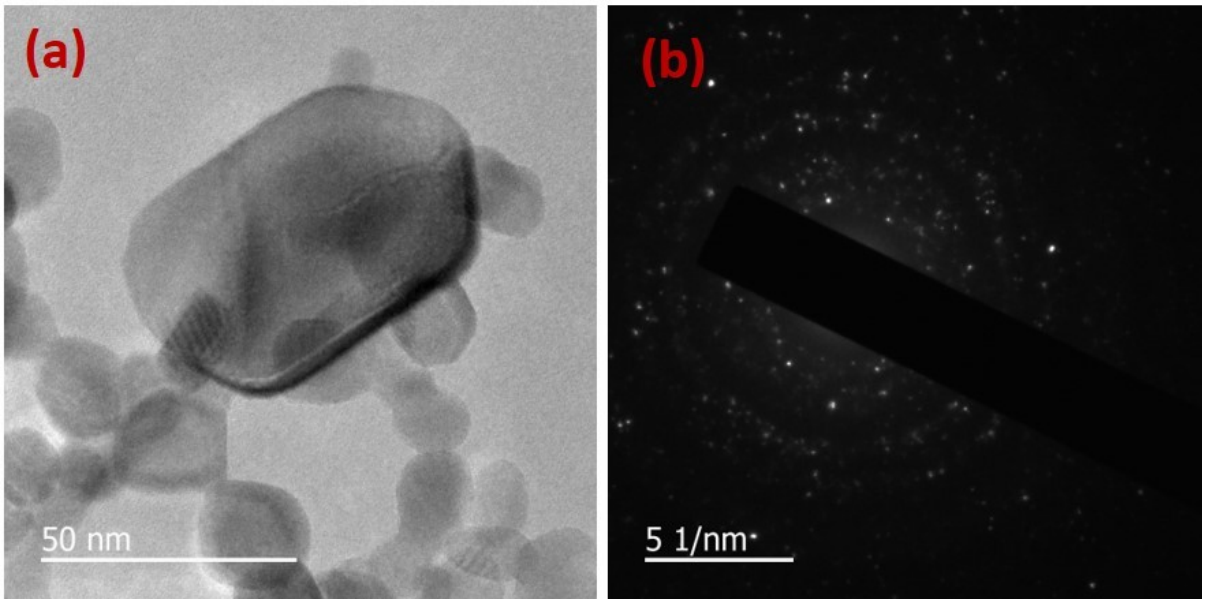

***Figure 5**. (a) TEM image of SnO_2 NPs (b) SAED pattern of the SnO_2 NP.*

4.2 EDX Analysis

In order to confirm the presence of elements in the developed SnO_2/AuNPs@SiNWs structure, EDX analysis was also performed where weight% and atomic% were observed as depicted in Fig.2(a). The elemental analysis also confirms the presence of Gold 'Au', oxygen 'O', Tin 'Sn' and silicon 'Si' species in the developed hybrid structures. The EDX mapping of the developed structure was also recorded as shown in Fig.3.

During the EDX measurement, the existence of four elements; Sn, Au, Si and O can be seen in the heterojunction nanostructure shown in colour mapping in Fig. 3. The atomic and weight percentage is shown in Fig.2(b). The atomic percentage of Oxygen is 17.91%, Silicon is 77.47%, Tin is 2.75% and of Gold is 1.88%. The EDX colour mapping of Gold, Oxygen and Tin shown in Fig. 3 show uniform coverage over the Silicon substrate.

4.3 XRD Diffractometer Analysis

XRD pattern of SnO_2 and SnO_2/AuNPs deposited over SiNWs on Si chip is shown in Fig. 4. The spectrum recorded for SnO_2 nanoparticles showed peaks at 2θ = 25.98°, 33.46°, 51.44° and 55.66° corresponding to (110), (101), (211) and (220) diffraction planes respectively [24]. The results are supported by JCPDS card no. 41-1445. The peaks of Au nanoparticles recorded at 2θ = 37.56°, 46.94° and 64.24° corresponding to (111), (200) and (220) diffraction planes respectively supported by JCPDS card no. 01-1172 [25].

4.4 TEM Analysis

The in-depth structural analysis of the prepared SnO_2 nanoparticle was done by using TEM as shown in Fig. 5(a). The samples were prepared on carbon coated copper grid after preparing the dispersion solution in ethanol where an ultrasonicator was used for ~ 45 min continuously to get a uniform distribution of the materials. Fig 5(b) shows the selected area electron diffraction patterns of the sample. The electron diffraction patterns show continuous ring patterns without any additional diffraction spots and rings of secondary phases, revealing their crystalline structure [24, 26]. XRD and TEM studies confirmed pure tetragonal structure of SnO_2 as evidenced from Fig. 5(a). The size of SnO_2 is of the order of 30-40nm.

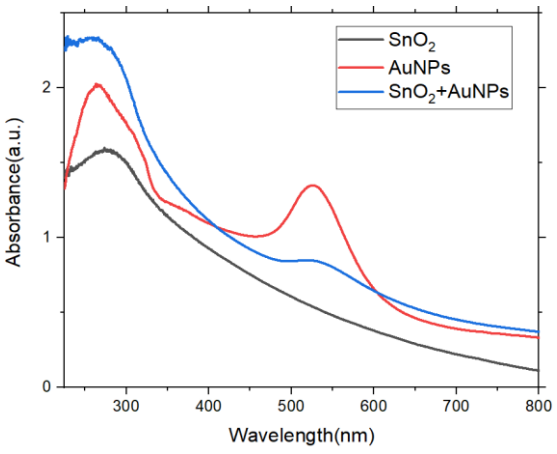

***Figure 6**. UV vis absorption spectra of SnO_2, AuNPs and SnO_2/AuNPs*

4.5 UV-Vis Analysis

Fig. 6 shows the UV-Vis spectra of SnO_2/AuNPs and SnO_2 samples. Because of the surface plasmon absorption (SPR) of the AuNPs mixed with SnO_2 sample, the SnO_2/AuNPs sample exhibits enhanced absorption in the UV-visible region with a very broad band around 550 nm[27]. Peak observation in the UV region occurs at 280 nm.

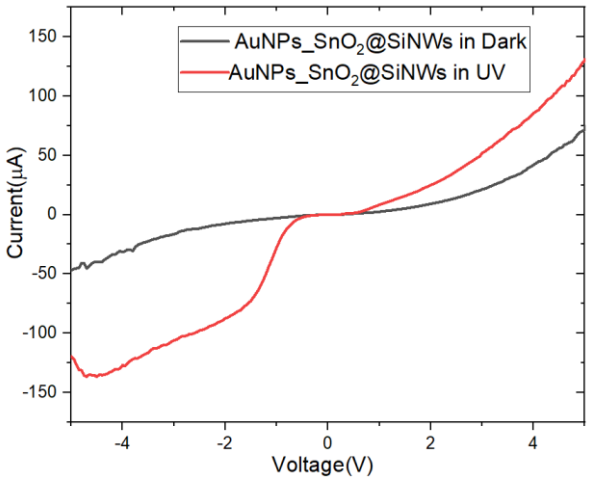

Figure 7. *I-V graph of SnO_2/AuNPs@SiNWs in dark and UV illumination*

4.6 UV response of the device

Here, in SnO_2/AuNPs deposited over SiNWs, we studied its I-V characteristics for dark condition and UV illumination condition. We can observe that in reverse bias condition the current in more than twice under UV illumination condition in comparison to dark condition shown in Fig. 7. Here the increase in current can be due to the SPR absorption of photons by Au nanoparticles.

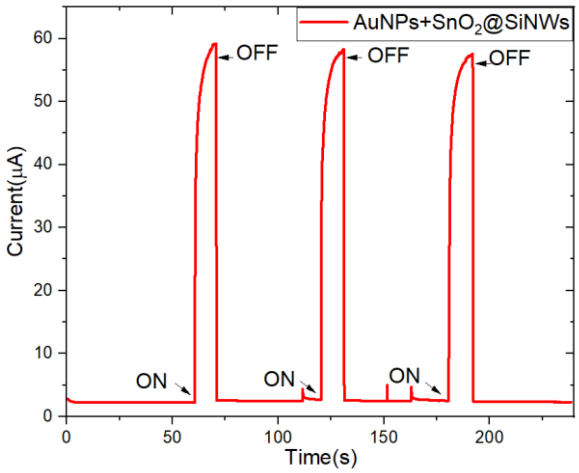

Figure 8. *I-t graph of SnO_2/AuNPs@SiNWs*

According to Liu et al. [28], graphene plasmons are generated when the energy of photons released from ZnO nanostructures is equal to the graphene surface plasmon energy. Hwang et al. [29] have reported similar results, demonstrating that improved photoemission from graphene/ZnO film architectures is caused by resonant stimulation of graphene plasmons. In our example, surface plasmons of Au nanoparticles are resonantly excited by photons emanating from nanostructured SnO_2.

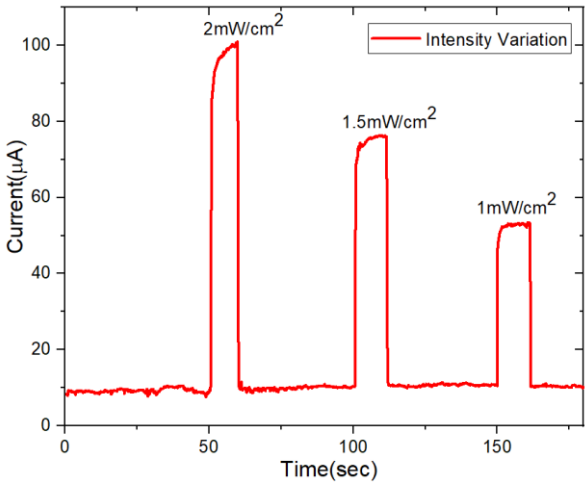

Figure 9. *Current in SnO_2/AuNPs@SiNWs with varying Intensity*

The powerful local light fields produced by these plasmons around the nanoparticles greatly intensify the incident light field [30]. These powerful electrons are transferred into the SnO_2 conduction band, increasing the conduction band electron density, and producing more UV emission as a result. Li et al. [31] examined surface plasmon effects on Au-ZnO films.

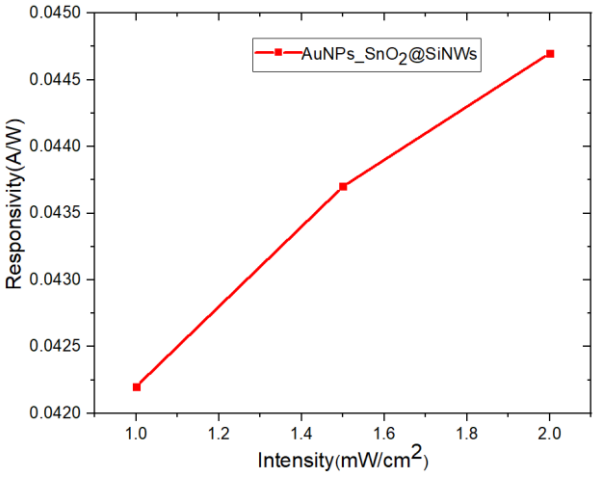

Figure 10. *Intensity vs Responsivity variation for SnO_2/AuNPs deposited over SiNWs*

In Fig. 8 we recorded 3 On/Off cycle of the current. Here, as we switch on the UV illumination

the current rises to ~ 58 μA and as we switch off the UV illumination very small dark current is observed. We also recorded the variation of on current with respect to time for different intensities of UV source, which is shown in Fig. 9. Here we recorded current for 2mW/cm^2, 1,5 mW/cm^2 and 1mW/cm^2.

We calculated responsivity of the device by using formula, Responsivity (R) = $\frac{I_{ph}}{P*A}$ A/W; where I_{ph} = I_L-I_d and calculated detectivity by using, Detectivity (D) = $\frac{R*A^{1/2}}{(2qI_d)^{1/2}}$ Jones [32]. Where, I_L= 9.98×10^{-5} A which is a current in presence of UV Radiation, I_d = 8.9×10^{-6} A i.e. current in dark, P = Power (2 mW), A= Area of device (1cm^2). By using above equations, the Responsivity and Detectivity was measured to be as, R = 45.4 × 10^{-3} A/W and D = 2.69 × 10^{10} Jones. The response time was measured to be ~ 1.32 s and decay time was ~ 0.77 s. The recovery of the device was found to be very fast. In Fig. 10, we recorded variation of responsivity with intensity. It is observed that responsivity increases with increasing intensity.

5. CONCLUSIONS

Here, a high-performance UV photodetector has been successfully fabricated by developing a heterojunction of SnO_2/AuNPs over SiNWs. SEM analysis depicts a uniform deposition of SnO_2/AuNPs over SiNWs which was supported by EDX color mapping and X-ray diffraction analysis. The TEM analysis of SnO_2 estimates the size of nanoparticles which is of the order of 30-40 nm. The developed UV photodetector revealed a good responsivity, detectivity and reproducibility under UV illumination where the responsivity and detectivity were estimated to be 45.4 × 10^{-3} A/W and 2.69 × 10^{10} Jones respectively with response time ~ 1.32 s and decay time ~ 0.77 s. Under different intensity, the photo current was observed to be decreasing with decrease intensity. Thus, developed heterojunction based device can be considered for future high-performance SiNWs based UV photodetectors that can be employed in a variety of applications due to its easy and inexpensive construction.

Acknowledgement

We thank Dr. Ashok K. Chauhan, founder president of Amity University, for his continuous support and also thanks to other members of the AIARS (M&D) group, Amity University, Noida for their support. The authors declared no financial conflict of interest.

REFERENCES

[1] Z.Alaie (2015) Recent advances in ultraviolet photodetectors. Materials Science in Semiconductor Processing, 29, 16-55. https://doi.org/10.1016/j.mssp.2014.02.054

[2] Z.Li (2023) Low-dimensional wide-bandgap semiconductors for UV photodetectors. Nature Reviews Materials, 8(9), 587-603. https://doi.org/10.1038/s41578-023-00583-9

[3] H.Chen (2015) New concept ultraviolet photodetectors. Materials Today, 18(9), 493-502. https://doi.org/10.1016/j.mattod.2015.06.001

[4] A.Kumar (2021) Recent advances in UV photodetectors based on 2D materials: A review. Journal of Physics D: Applied Physics 55(13), 133002. https://iopscience.iop.org/article/10.1088/1361-6463/ac33d7/meta.

[5] Z. Lou (2016) Flexible photodetectors based on 1D inorganic nanostructures. Advanced Science 3.6, 1500287. https://doi.org/10.1002/advs.201500287

[6] J. Son (2018) UV detectors: status and prospects. UV and Higher Energy Photonics: From Materials to Applications 2018 10727, 12-20. https://doi.org/10.1117/12.2324105

[7] E. Munoz (2001) III nitrides and UV detection. Journal of Physics: Condensed Matter 13, no. 32, 7115. https://iopscience.iop.org/article/10.1088/0953-8984/13/32/316/meta

[8] L. Shi (2012) Comparative study of silicon-based ultraviolet photodetectors. IEEE Sensors Journal 12.7, 2453-2459 DOI: 10.1109/JSEN.2012.2192103

[9] F. Bouzid (2018) Numerical simulation study of a high efficient AlGaN-based ultraviolet photodetector. Superlattices and microstructures 122, 57-73. https://doi.org/10.1016/j.spmi.2018.08.022.

[10] Z. Li (2022) Application of nanostructured TiO2 in UV photodetectors: A review. Advanced Materials 34, no. 28, 2109083. https://doi.org/10.1002/adma.202109083

[11] J. Chen (2020) Recent progress of heterojunction ultraviolet photodetectors: materials, integrations, and applications. Advanced Functional Materials 30, no. 16, 1909909. https://doi.org/10.1002/adfm.201909909

[12] P. Chetri (2019) Self-powered UV detection using SnO2 nanowire arrays with Au Schottky contact. Materials Science in Semiconductor Processing 100, 123-129. https://doi.org/10.1016/j.mssp.2019.05.003

[13] A. Gundimeda (2017) Fabrication of non-polar GaN based highly responsive and fast UV photodetector. Applied Physics Letters 110, no. 10. https://doi.org/10.1063/1.4978427

[14] M. Zhong (2015) High-performance single crystalline UV photodetectors of β-Ga2O3. Journal

of Alloys and Compounds 619, 572-575. https://doi.org/10.1016/j.jallcom.2014.09.070

[15] U.M. Nayef (2016) Ultraviolet photodetector based on TiO2 nanoparticles/porous silicon hetrojunction. Optik 127.5, 2806-2810. https://doi.org/10.1016/j.ijleo.2015.12.002

[16] J.L. Yang (2017) Recent progress of ZnMgO ultraviolet photodetector. Chinese Physics B 26.4, 047308. https://iopscience.iop.org/article/10.1088/1674-1056/26/4/047308/meta

[17] C.A. Amarnath (2013) Nanohybridization of low-dimensional nanomaterials: synthesis, classification, and application. Critical reviews in solid state and materials sciences 38, no. 1, 1-56. https://doi.org/10.1080/10408436.2012.732545

[18] P. Singh (2022) Development of an ultrasensitive IR sensor using ZnO/SiNWs hybrid nanostructure. Materials Today: Proceedings 66, 2303-2307. https://doi.org/10.1016/j.matpr.2022.06.229

[19] A. Kumar (2020) Fabrication of SiNWs/Graphene nanocomposite for IR sensing. Materials Today: Proceedings 32, 397-401. https://doi.org/10.1016/j.matpr.2020.02.086

[20] M. Iqbal (2016) Preparation of gold nanoparticles and determination of their particles size via different methods. Materials Research Bulletin 79, 97-104. https://doi.org/10.1016/j.materresbull.2015.12.026

[21] T. Muangnapoh (2010) Facile strategy for stability control of gold nanoparticles synthesized by aqueous reduction method. Current Applied Physics 10, no. 2, 708-714. https://doi.org/10.1016/j.cap.2009.09.005

[22] M.V. Arularasu (2018) Structural, optical, morphological and microbial studies on SnO2 nanoparticles prepared by co-precipitation method. Journal of nanoscience and nanotechnology 18, no. 5, 3511-3517. https://doi.org/10.1166/jnn.2018.14658

[23] X. Cui (2017) The synthesis of polyamidoamine modified gold nanoparticles/SnO2/graphene sheets nanocomposite and its application in biosensor. Colloids and Surfaces A: Physicochemical and Engineering Aspects 520, 668-675. https://doi.org/10.1016/j.colsurfa.2017.02.030

[24] A. Borhaninia (2017) Gas sensing properties of SnO2 nanoparticles mixed with gold nanoparticles. Transactions of Nonferrous Metals Society of China 27.8, 1777-1784. https://doi.org/10.1016/S1003-6326(17)60200-0

[25] J.Y. Cheong (2017) In situ high-resolution transmission electron microscopy (TEM) observation of Sn nanoparticles on SnO2 nanotubes under lithiation. Microscopy and Microanalysis 23, no. 6, 1107-1115. https://doi.org/10.1017/S1431927617012739

[26] Y. Wang (2016) Facile approach to synthesize uniform Au@ mesoporous SnO 2 yolk–shell nanoparticles and their excellent catalytic activity in 4-nitrophenol reduction. Journal of Nanoparticle Research 18, 1-11. https://doi.org/10.1007/s11051-015-3307-8

[27] M. Ivanovskaya (2021) Effect of Au nanoparticles on the gas sensitivity of nanosized SnO2. Materials Chemistry and Physics 258, 123858. https://doi.org/10.1016/j.matchemphys.2020.123858

[28] R. Liu (2013) Graphene plasmon enhanced photoluminescence in ZnO microwires, Nanoscale 5, 5294. https://doi.org/10.1039/C3NR01226C

[29] S.W. Hwang (2010) Plasmon-enhanced ultraviolet photoluminescence from hybrid structures of graphene/ZnO films, Phys. Rev. Lett. 105, 127403. https://doi.org/10.1103/PhysRevLett.105.127403

[30] B. Lamprecht (2001) Surface plasmon propagation in microscale metal stripes, Appl. Phys. Lett. 79, 51–53. https://doi.org/10.1063/1.1380236

[31] X. Li (2009) Effects of localized surface plasmons on the photoluminescence properties of Au-coated ZnO films, Optics Exp. 17, 8737–8740. https://doi.org/10.1364/OE.17.008735

[32] G. Wang (2018) Two dimensional materials based photodetectors, Infrared Physics & Technology, 88, 149–173. https://doi.org/10.1016/j.infrared.2017.11.009

IZVOD

RAZVOJ UV FOTODETEKTORA KOJI KORISTI SNO_2/AUNPS@SINWS HETEROSPOJNICU NA SI ČIPU

U ovoj studiji predstavljen je razvoj hibridne nanostrukture zasnovane na silicijumskim nanoosnovi (SiNV) i nanočesticama kalajnog oksida (SnO_2) i Au, koja je korišćena za razvoj UV fotodetektora. Hemijsko jetkanje uz pomoć metala (MACE) korišćeno je za kreiranje SiNV na p -Si (1 1 1) supstratu, dok su tehnike redukcione sinteze i ko-precipitacije korišćene za stvaranje AuNP i SnO_2 nanočestica, respektivno. Ove nanočestice AuNP i SnO2 su zatim deponovane na SiNV. Koristeći rendgenski difraktometar (XRD), UV-vidljivi spektrofotometar i skenirajuću elektronsku mikroskopiju (SEM), ispitana je sintetizovana hibridna nanostruktura SnO_2/AuNPs@SiNWs. Sintetizovane nanočestice SnO_2 su, takođe, podvrgnute TEM ispitivanju. Na sobnoj temperaturi, UV fotostrujni odgovor SnO_2/AuNPs@SiNWs je proučavan pri različitim intenzitetima UV svetlosti od 1, 1,5 i 2 mV/cm2. Utvrđeno je da hibridna nanostruktura SnO_2/AuNPs@SiNWs ima vreme odziva fotostruje veoma brzo (1,32 s). Kako smo isključili UV izvor, senzor je dostigao svoje početno stanje za ~0,77 s. Uzorak je kontinuirano proveravan za tri uključena /isključena seta osvetljenja u redovnom intervalu od 60 s. Stoga, rad koji je ovde otkriven ima veliko obećanje za unapređenje visoko efikasnih minijaturnih UV fotodetektora sa jedinstvenim karakteristikama.
Ključne reči: *Fotodetektor, ultraljubičasto, nanočestice zlata, silicijumske nanožice, kalaj oksid.*

Naučni rad
Rad primljen: 16.09.2024.
Rad prihvaćen: 02.12.2024.

Pooja Singh: https://orcid.org/0000-0001-8370-5775
Dr. Avshish Kumar: https://orcid.org/0000-0003-1681-5426
Dr. V.K. Jain: https://orcid.org/0000-0002-4439-6583